BIOELECTRICITY
Volume 2, Number 2, 2020

DOI: 10.1089/bioe.2020.0010

Review

Polypyrrole-Incorporated Conducting Constructs for Tissue Engineering Applications: A Review

Yeshi Liang, BE[1] and James Cho-Hong Goh, PhD[1,2]

Abstract

Conductive polymers have recently attracted interest in biomedical applications because of their excellent intrinsic electrical conductivity and satisfactory biocompatibility. Polypyrrole (PPy) is one of the most popular among these conductive polymers due to its high conductivity under physiological conditions, and it can be chemically modified to allow biomolecules conjugation. PPy has been used in fabricating biocompatible stimulus-responsive scaffolds for tissue engineering applications, especially for repair and regeneration of electroactive tissues, such as the bone, neuron, and heart. This review provides a comprehensive overview of the basic properties and synthesis methods of PPy, as well as a summary of the materials that have been integrated with PPy. These composite scaffolds are comparatively evaluated with regard to their mechanical properties, biocompatibility, and usage in tissue engineering.

Keywords: polypyrrole, conductive tissue engineering, conductive scaffold

Introduction

One of the critical objectives in tissue engineering is to mimic the extracellular matrix (ECM) of the targeted tissue with regard to its intrinsic architecture, chemical and biological properties.[1,2] Therefore, scaffolds made of different biomaterials, through a variety of fabrication methods, have been extensively studied to determine the suitable mechanical properties and biomimetic architecture. In addition, the biochemical properties of the surface of the scaffolds are enhanced through the integration of biomolecules and proteins. Growth factors, with controlled release, can also be included to promote cell adhesion as well as proliferation, further growth, and induce differentiation.[3] In electroactive tissues such as the nerve, bone and cardiac tissues, which possess intrinsic conductive properties, bioelectricity modulates the fate and behavior of cells through various biological pathways.[4,5] Consequently, in addition to providing similar structure, mechanical and biochemical properties to the native ECM, it is believed that the successful engineering of these electroactive tissues requires scaffolds to be conductive themselves.[6] Traditional scaffolds made of insulated materials block vital cell–cell signaling, inhibiting tissue regeneration. Hence, it is necessary to have a scaffold with the ability to deliver electrical signals for these electrically responsive cells.

In previous years, various conductive materials were explored to fabricate scaffolds, such as gold-based particles and carbon-based particles.[7,8] These materials were either used purely or incorporated with other materials as a composite. It has been shown that these scaffolds, with electrically conductive materials, were able to promote cell adhesion, migration, proliferation, and differentiation, mainly when used for electroactive cells.[9] However, most of these materials have drawbacks, such as the high cost of gold materials that restricts their usage on large-scale fabrication; and the potential cytotoxicity of carbon-based materials that limits their applications on implantable scaffolds.[10] In the mid-1970s, the first conductive polymer was synthesized, for which the Nobel Prize in Chemistry was jointly awarded to three scientists responsible for its discovery and development.[11] Conductive polymers are functionally versatile—they possess the mechanical properties and ease of fabrication known to polymers, and the electrical conductivity similar to metals and semiconductors.[12] Thus, they have been utilized in different applications, such as actuators, batteries, and microelectronics.[6] Recently, conductive polymers were explored for biomedical applications due to their biocompatibility, conductivity, reversible oxidation, redox stability, and hydrophobicity, which are desirable properties for tissue engineering.[13]

The success of growing mammalian cells on scaffolds made of polyacetylene, a conductive polymer, demonstrated

Departments of [1]Biomedical Engineering and [2]Orthopedic Surgery, National University of Singapore, Singapore.

the potential of such polymers in tissue engineering.[14] To this date, more than 25 additional conductive polymers have been developed and used in biomedical applications, such as polypyrrole (PPy), polyaniline, polythiophene, and poly(3,4-ethylenedioxythiophene) (PEDOT).[15] PPy is one of the most extensively utilized conductive polymers in tissue regeneration. It has been incorporated into various materials, via different polymerization and fabrication methods, to enhance scaffold properties and promote cell functions. It was reported that PPy-based materials exhibit levels of immunogenicity that are comparable to other FDA-approved biomaterials.[10] Accordingly, researchers have applied PPy-containing composites in the regeneration of electroactive tissues as alternative approaches to solve clinical problems besides current treatments.

In this review, a brief introduction of PPy is given, followed by an overview of current approaches used to synthesize conductive PPy from pyrrole (py) monomers. Subsequently, a summary of the different materials that PPy has been incorporated into is provided. Then, it gives a comparative analysis of the use of these PPy-containing scaffolds in neural, bone, and cardiac tissue engineering. In particular, it includes the effects of using a conductive scaffold together with and without external electrical stimulation on cell behavior; as well as the hypothesized molecular mechanism on how conductive PPy material communicates with cells. Current challenges and future directions of using PPy-containing composites in tissue regeneration are pointed out in the end.

Conductive Polymers

Unlike metal, polymers are not usually electrically conductive because the electrons of polymers are not delocalized. Therefore, electrons cannot flow easily from atom to atom to conduct currents. However, the conjugated backbone, wherein the carbon atoms are connected alternatively with single bonds and double bonds, of the conductive polymers, makes them possibly conductive.[16] The single bond contains a strong chemically localized σ-bond, which also appears in the double bond.[17] The other bond inside a double bond is a localized π-bond, which is not as strong as the σ-bond.[18] This weaker localized π-bond allows the electrons to be more easily delocalized and to jump between the chains of the polymer.[19,20] Thus, the system becomes unstable and will induce the formation of an energy gap, which requires the dopant ions to be overcome.[21] A dopant is usually a negatively charged ion that is used to stabilize the oxidized polymers, and it plays a key role in conduction. Under an electric potential, dopants on the polymer backbone start to move, transforming the atoms to polarons or bipolarons. Charges are then allowed to be passed, and this renders conductivity to the polymer.[15,17,21,22]

The polymerization process to fabricate conductive polymers can be divided into two processes: chemical polymerization and electrochemical polymerization.[23,24] Chemical polymerization allows bulk production by mixing the monomer solution and an oxidizing agent, such as ferric chloride ($FeCl_3$) and ammonium persulfate (APS), together (Fig. 1). It is also known as *in situ* polymerization, wherein the dopant is usually included to maintain the conductivity. In electrochemical polymerization, the electrical current applied on the electrodes, soaking in the mixture of monomer, solvent, and the doping agent, leads to the attachment and oxidization of monomer on the positively charged electrode. The former way is suitable for all conductive polymer fabrication. However, only powder and thick films can be achieved.[25] In comparison, electrochemical polymerization can produce conductive polymer films as thin as 20 μm. One disadvantage of electrochemical polymerization is that the final products can hardly be modified, whereas it is still possible to do covalent modification on the backbone of these conductive polymers.[15,21]

Polypyrrole

The chemical structure of PPy consists of repeating units of the py monomer, a nitrogen-containing aromatic ring. The

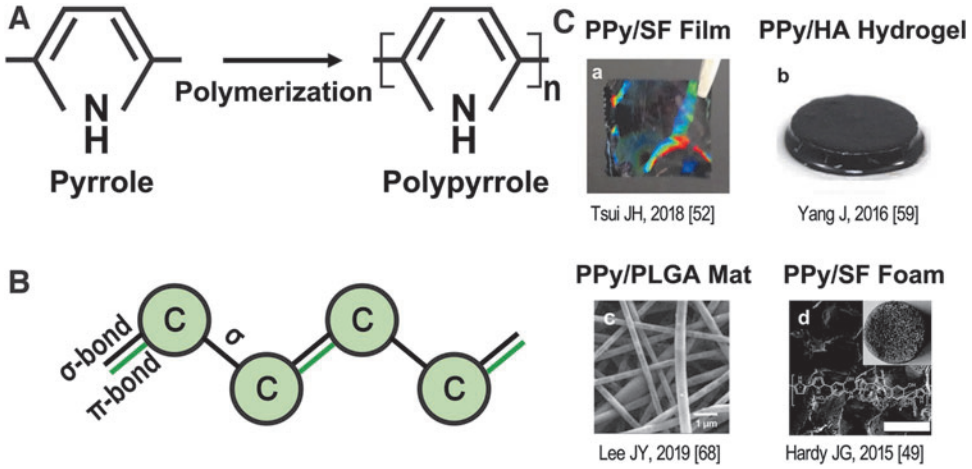

FIG. 1. **(A)** Polymerization of PPy from pyrrole monomers using $FeCl_3$ as oxidant. Oxidation of pyrrole using $FeCl_3$: $nC_4H_4NH + FeCl_3 \rightarrow (C_4H_2NH)n + FeCl_2 + HCl$; oxidation (p-doping) of the PPy with dopant in the system to maintain PPy conductivity: $(C_4H_2NH)n + xFeCl_3 \rightarrow (C_4H_2NH)nCl + xFeCl_2$. **(B)** Illustration of the conjugated backbone of conductive polymer; alternating pattern of double and single bonds in the backbone. Black bond represents Sigma-bond, which strengthens the electrons; green bond represents the Pi-bond, which exists in the double bond, with lower strength. **(C)** Incorporation of PPy with different materials as scaffolds. **(a)** PPy/SF film; **(b)** PPy/HA hydrogel; **(c)** PPy/PLGA mat; **(d)** PPy/SF foam. $FeCl_3$, ferric chloride; PPy, polypyrrole; SF, silk fibroin; HA, hyaluronic acid; PLGA, poly(lactic-co-glycolic acid).

mechanism of py polymerization is under debate. Still, it most likely involves complex reactions, including oxidation, deprotonation, and crosslinking.[26] The doping process of PPy is p-doping, where the polymer is oxidized and will have a positive charge.[15,27] One of the two leading theories is that py monomers are first oxidized to release a radical cation, followed by the coupling of two cations and the production of a bipyrrole.[26] As oxidation continues, the chain continues to grow. On the other hand, the second theory advocates that a cation reacts with a neutral monomer. After oxidation and deprotonation, a dimer is formed, and the polymer chains keep growing by repeating this process.[28,29] Eventually, a conduction band is developed by the delocalized electrons from the double bond in the backbone of the PPy, resulting in metallic behavior.[21]

PPy exhibits good electrical conductivity under physiological conditions due to its p-type conduction. It is biocompatible and can be chemically modified to be better conjugated with biomolecules. Moreover, it can be easily synthesized through both electrochemical polymerization and chemical polymerization.[30,31] Despite the advantages of PPy, it has some properties that prohibit its use in tissue engineering. First, its brittleness makes it inappropriate for nonrigid tissue applications.[32] Second, it cannot be easily used in some traditional scaffold fabrication methods, such as electrospinning, due to its poor solubility.[6,33] Lastly, since it is mostly nondegradable, it is challenging to use it to fabricate degradable scaffolds, which is usually desired for regenerative medicine.[34] To tackle these drawbacks, studies have been done on incorporating PPy into both natural and synthetic biomaterials. Composite materials have the advantages of tailoring the material properties by adjusting the ratio among the materials. Another approach that has been investigated is to deposit conductive polymers onto a polymer with superior mechanical properties, to take advantage of its mechanical properties while increasing the conductivity.[1,6]

Incorporation of PPy to Other Materials

In the next section, we discuss constructs made of a combination of PPy and different materials (Fig. 1 and Table 1) in terms of fabrication methods, changes in chemical structures, surface morphology, mechanical properties, electrical conductivity, and degradation behavior.

Conjugation with natural materials

Chitosan. Chitosan (CHI) is a linear polysaccharide mainly obtained from chitin, the fundamental component of crustacean shells.[35] The primary amines along the backbone of CHI give it excellent biocompatibility and biodegradability.[36] In biomedical applications, CHI usually appears in crosslinked hydrogel form.

PPy has been successfully immobilized in CHI in many studies and mostly through oxidative chemical polymerization. CHI/PPy injectable hydrogel was explored by Cui et al., as shown in Figure 2A and B.[37] They first mixed a py monomer with CHI dissolved in 1% (v/v) acetic acid; then, $FeCl_3$ was added to initiate the polymerization. Free amino groups (-NH2) in the mixture were crosslinked with aldehyde groups of glutaraldehyde to get CHI/PPy hydrogel. They found that CHI/PPy composite with a lower amount of chitosan did not form a hydrogel, possibly due to fewer available functional groups on the backbone of CHI. A similar method, but dialysis against water, was used by He et al. to fabricate gelfoam as a patch for cardiac repair.[38] Lastly, Bu et al. added presynthesized PPy powder to sodium alginate (SA)/carboxymethyl chitosan (CM-CHI) and used Ca^{2+} to trigger the formation of clathrates (Fig. 2).[39] All the specific Fourier Transform Infrared (FTIR) spectra peaks, including bands at $1033\,cm^{-1}$ of PPY and an enhanced peak of C-N from SA/CM-CHI at $1126\,cm^{-1}$, were present in the SA/CM-CHI/PPy hydrogel, verifying the successful synthesis of PPy/CHI hydrogel.

In terms of mechanical properties, the addition of PPy resulted in a slight decrease in tensile strength and Young's modulus compared with the pure SA/CM-CHI hydrogel. This was mainly due to the dominant influences of the inherent structural brittleness of PPy, and the limited support of the dispersed PPy particles on the structure of the whole hydrogel. Interestingly, there was a slowly increasing trend in both tensile strength, from 0.038 to 0.065 MPa, and Young's modulus, from 0.175 to 0.406 MPa, with an increasing mass of PPy, from 0.02 to 0.4, in the SA/CM-CHI/PPy hydrogel. The mechanical properties of SA/CM-CHI/PPy(0.4) were closest to those of SA/CM-CHI. This phenomenon was postulated to be due to the positively charged PPy that interacts with the hydrogel's basic skeleton through electrostatic interactions and thus promoted the mechanical and structural stability of the SA/CM-CHI/PPy hydrogels.[39] In line with this, He et al. found that the maximum strain was reduced in CHI/PPy hydrogels compared with pure CHI hydrogel, but the mean breaking stress was significantly higher.[38] Therefore, these results proved that by combining CHI with PPy, the brittleness could be reduced.

Regarding conductivity, the primary trend is that conductivity increases as more PPy in the composite. He et al. used a two-probe conductive analyzer with a linear double-sweep model for measurement.[38] They found that CHI/PPy hydrogels formed hysteresis loops. In contrast, CHI hydrogels demonstrated a uniform linear relationship, representing a significantly higher conductivity in CHI/PPy patches than CHI patches. Bu et al. also found two oxidation peaks and two reduction peaks from the cyclic voltammetry of the PPy-containing hydrogel, which indicated its excellent electrochemical activity.[39] Moreover, the four-point probe method results showed that the addition of PPy increased the conductivity from 7.35×10^{-6} S/cm of CHI hydrogel to 8.03×10^{-3} S/cm of SA/CM-CHI/PPy(0.4).

Degradation of the composites was evaluated by Bu et al. comparing the morphological changes after soaking the samples in phosphate-buffered saline (PBS) for 3 and 6 weeks.[39] They found that there were no significant morphological changes of SA/CM-CHI/PPy in 3 weeks, but some of the PPy particles attached to the interior of the hydrogel were exposed. After 6 weeks, some parts of the SA/CM-CHI/PPy hydrogel exhibited evident collapse and fracture. However, no comparison was made against pure SA/CM-CHI. They suggested that the SA/CM-CHI/PPy hydrogel is biodegradable and has the potential to be used as an internal filling material for nerve conduit that degrades within a short period.

Alginate. Extracted from brown seaweeds, alginate (ALG) is a naturally occurring anionic polymer.[40] It is composed of glucuronic acid and mannuronic acid. Hence, it

Table 1. Summary of Polypyrrole-Containing Scaffolds Used in Tissue Engineering and Their Formats, Properties, and Performances

Main material	*Scaffold format*	*PPy incorporation*	*Dopant/oxidant*	*Concentration*	*Electrical properties*	*Cell sources and usages*	In vitro/vivo *results*	*Ref.*
ALG	Crosslinked hydrogel	Immerse coating	N.A./$FeCl_3$	[py]: 0–20×10^{-3} M	py[10]/ALG: 1.1 $\pm0.3\times10^{-4}$ S/cm	*In vivo* model/NTE	PPy/ALG hydrogels enhanced expression of Tuj1 and MAP2. Mild inflammatory reactions after 8 weeks of implantation.	43
ALG/COL	Crosslinked hydrogel	Mix ALG/COL with doped PPy	HCl/$FeCl_3$	ALG-graft-PPy: ALG (wt%): 20:80, 30:70	20%: 220 mS/cm 30%: 229 mS/cm	hMSCs/ biocompatibility	No cytotoxicity effects.	9
ALG/CHI	Crosslinked hydrogel	Mix ALG/CHI with doped PPy	HCl/APS	PPy: 0.02–0.4 g	7.35×10^{-6}–8.03×10^{-3} S/cm	PC12, RSC96, BMMSC/NTE	SA/CMCS/PPy hydrogels supported cell growth and proliferation. No severe inflammatory tissue responses when implanted *in vivo*. Better nerve fibers morphology in SA/CMCS/PPy hydrogels than the autologous nerve group.	39
ALG/CHI	Doubled lyophilized foam	Mix ALG/CHI with py, then polymerize	HCl/$FeCl_3$	[py]: 0.1 M	550–1000 nA	MG-63/BTE	CHI/PPy/ALG scaffold promoted the formation of apatite layer.	44
CHI	Crosslinked hydrogel	Mix CHI with py, then polymerize	N.A./$FeCl_3$	[PPy]: 0.04%	N.A.	NRCM/CTE	Synchronous contraction of two distinct clusters of CMs connected by PPy/CHI composite. Higher EMG signal amplitude in scar tissue from PPy/CHI-treated animals.	37
CHI	Crosslinked gelfoam	Mix CHI with py, then polymerize	N.A./$FeCl_3$	N.A.	12.5×10^{-5} S/cm	NRCM/CTE	Higher calcium transient velocity of CMs on PPy composite. Faster conduction velocity on the epicardial surface of PPy composite-implanted hearts.	38
COL	IPC-mesh	Immerse coating	Cl^-/$FeCl_3$	N.A.	N.A.	hMSC/NTE	Upregulated expression of noggin, MAP2, neurofilament, β tubulin III, and nestin from hMSCs on PPy/COL scaffolds.	62
COL	Hybrid microfibers hydrogel	Mix synthesized PPy with COL	N.A./$FeCl_3$	[PPy]: 0–1 mg/mL [COL]: 6 mg/mL	Col 0.5: 0.22 S/m	PC12/NTE	Enhanced electroconductivity in PPy/COL hydrogel microfibers. Improved PC12 cells neurogenesis.	63

(*continued*)

Table 1. (Continued)

Main material	*Scaffold format*	*PPy incorporation*	*Dopant/oxidant*	*Concentration*	*Electrical properties*	*Cell sources and usages*	In vitro/vivo *results*	*Ref.*
COL/PAR	Inkjet-printed scaffold	Print on top of PPy lines	PVA/$FeCl_3$, FepTS	py: 136 mg	1.1 S/cm	PC12/NTE	Promoted neurite outgrowth and orientation on PPy/COL scaffold with electrical stimulation.	70
GX	Hydrogel	Electrochemically polymerization	GX/N.A.	[Py]: 0.4 M	Voltammetric peak: 0.2 (ox), –0.3 V (red)	Human fibroblast	Better cell adhesion on PPy/GX scaffold. External magnetic field helped cell adhesion and proliferation.	61
SF	Lyophilized foam	Immerse coating	HCl/APS	[py]: 14.28 mM	N.A.	hMSC/BTE	Increased collagen production of the hMSCs on PPy/SF scaffolds.	49
SF	Acid modified film	Immerse coating	p-TSA/$FeCl_3$	[py]: 50 mM	200–500 Ω/sq	hESC-derived CMs/CTE	Anisotropic topographical cues led to increased cellular organization and sarcomere development. Electroconductive cues promoted CX43 expression and polarization.	52
SF	3D print and electrospinning composite	Immerse coating	HCl/$FeCl_3$	[py]: 14 mM	1×10^{-5}–1×10^{-3} S/cm	Mouse fibroblasts, SCs/NTE	No cytotoxicity and did not affect SC proliferation.	1
SF	Electrospun mat	Immerse coating	NaCl/$FeCl_3$	[py]: 0.3 M	Similar voltammograms to free-standing PPy	hMSC, hfibroblasts/ Biocompatibility	No cytotoxicity and supported cell proliferation *in vitro*.	50
HA	Hydrogel	Immerse coating	N.A./APS	[py]: 0–100 Mm	10^{-3}–10^{-2} S/cm	3T3/Biocompatibility	PPy/HA composites supported cell attachment and proliferation.	59
HA/GEL	Self-adhesive hydrogel	Paint dopa-PPy on dopa-Gel/HA	N.A./$FeCl_3$	[dopa-PPy]: 0–0.6% [dopa-Gel]: 25%	$1.09\pm0.06\times10^{-6}$ -2.85 ± 0.18 $\times10^{-4}$ S/cm	*In vivo* model/CTE	Dopa-Gel/PPy hydrogel could tightly adhere to the porcine myocardium. Smaller infarct sizes and thicker left ventricle walls.	60
HAp	Lyophilized foam	Mix HAp with doped PPy	N.A./N.A.	ppy: 0.26% w/v	N.A.	Osteoblast/BTR	Higher protein adsorption and drug release rate over a long period in PPy contained composites.	69
PCL	Film	Immerse coating	p-TSA/$FeCl_3$	[py]: 0.084 M	1.0 ± 0.4 kΩ cm	HL1/CTE	Higher calcium wave propagation and shorter transient duration on PPy/PCL composites.	10
PCL	Electrospunelectrospray mat	py vapor	p-TSA/$FeCl_3$	Oxidant electrospraying time: 1–4 h	1.3–1.9 S/cm	L929/Biocompatibility	PPy/PCL scaffold promoted PC12 attachment or proliferation.	65
PCL	Rolled 3D-printed scaffold	Mix PPy-block-PCL with PCL pellets	N.A./N.A.	[PPy-b-PCL]: 0.5–2%, PCL: 70%	0.28 ± 0.02–1.15 ±0.03 mS/cm	hESC-derived NSCs/NTE	PCL/PPy scaffold enhanced cell maturation toward peripheral neuronal cells.	66

(*continued*)

TABLE 1. (CONTINUED)

Main material	*Scaffold format*	*PPy incorporation*	*Dopant/oxidant*	*Concentration*	*Electrical properties*	*Cell sources and usages*	In vitro/vivo *results*	*Ref.*
PCL/GEL	Electrospun mat	Disperse doped PPy in spinning solution	N.A./N.A.	PPy/PCL-GEL (PPG): 15:85, 30:70	PPG15: 0.013 mS/cm PPG30: 0.37 mS/cm	Rabbit primary CM/CTE	Higher expression of CX43 in PPy/PCL scaffolds.	13
PLCL/SF	Electrospun mat	Immerse coating	p-TSA/$FeCl_3$	[py]: 2 M, volume: 0–50 μL	8.52×10^{-6}–1.36×10^{-4}	*In vivo* model/NTE	PPy/PLCL/SF mat promoted SCs proliferation *in vivo*. Thicker myelin in regenerated nerve and better sciatic nerve function recovery.	6
PCL/PSS	Electrospun mat	Immerse coating	N.A./$FeCl_3$	[py]: 84 mM	52.8 ± 4.7 kΩ/sq	hMSCs/BTE	Increased ALP expression and calcium deposition on PPy/PCL/PSS scaffolds both with and without electrical stimulation.	64
PGA	Thermosetting injectable spring	Immerse coating after dopamine treatment	N.A./$FeCl_3$	[PY]: 0.2 M	80.84 S/m	HUVECs, RAECs, *in vivo* model/CTE	Highly oriented sarcomeres. Enhanced CM's maturation in synchronous contraction. Decreased ventricle infarct size.	94
PLA	Electrospun mat	Mix synthesized PPy in spinning solution	p123/$FeCl_3$	[PPy]: 1.8% [PLA]: 12.5%	N.A.	*In vivo* model/NTE	PPy/PLA nanofibrous scaffold inhibited scar tissue formation. Induced the axonal regeneration and myelination in the lesion area.	79
PLA	Electrospun mat	Mix synthesized PPy in spinning solution	p123/$FeCl_3$	[PPy]: 15%	1.10×10^{-4} S/cm	*In vivo* model/NTE	Six weeks after injury, the use of PLA/PPy scaffolds significantly reduced the activation of astrocytes and increased axonal regeneration.	80
PLA/PLO	Electrospun mat	Disperse doped PPy in spinning solution	N.A./N.A.	PPy:PLA (wt/wt): 1–10	N.A.	PC12/NTE	PPy-containing scaffolds supported PC12 cells differentiation without electrical stimulation, which could be further enhanced with electrical stimulation.	4
PLGA	Micro-grooved scaffold	Immerse coating	NaCl/$FeCl_3$	[py]: 2.875, 5.75, 11.5 mM	9.63–38.56 S/cm	mNSCs/NTE	Enhanced mNSCs neuronal differentiation on PPy-coated microgroove scaffolds even without electrical stimulation, which was further enhanced with electrical stimulation.	77

(*continued*)

Table 1. (Continued)

Main material	*Scaffold format*	*PPy incorporation*	*Dopant/oxidant*	*Concentration*	*Electrical properties*	*Cell sources and usages*	In vitro/vivo *results*	*Ref.*
PLGA	Electrospun mat	py vapor, electrochemical polymerization	NaDBS/$FeCl_3$	[py]: 0.1 M	N.A.	iPSC/CTE	iPSCs on conductive scaffolds showed elevated expression of Actinin, NKX2.5, GATA4, and Myh6 both stimulated and unstimulated.	67
PLGA	Electrospun mat	Immerse coating	pTS/$FeCl_3$	[py]: 14 mM	$7.4 \pm 3.2 \times 10^3$–$9.0 \pm 6.0 \times 10^4$ Ω/sq	PC12/NTE	PPy/PLGA meshes supported differentiation of PC12. Longer neurites on conductive scaffold with electrical stimulation than nonstimulated ones.	68
PGS/COL	Film	Mix PPy with PGS/Col solution	N.A./N.A.	[COL]: 0%, 0.5% [PPy]: 0–5%	COL 0.5–PPy 5: 0.06 ± 0.14 S/cm	H9C2/CTE and drug release	PPy and collagen improved scaffolds' protein adsorption ability. 5% PPy did not change the degradation speed of the patch. Drug-loaded film promoted cell proliferation till 21 days.	95

ALG, alginate; ALP, alkaline phosphatase; APS, ammonium persulfate; BMMSC, bone marrow mesenchymal stem cell; BTE, bone tissue engineering; CHI, chitosan; CM, cardiomyocyte; CMCS, carboxymethyl chitosan; COL, collagen; CTE, cardiac tissue engineering; CX43, Connexin 43; dopa, dopamine; $FeCl_3$, ferric chloride; FepTS, ferric p-toluene sulfonate; GEL, gelatin; HA, hyaluronic acid; HAp, synthetic hydroxyapatite; HCl, hydrochloric acid; hESC, human embryonic stem cell; hMSCs, human mesenchymal stem cells; HUVECs, human umbilical vein endothelial cells; IPC, interfacial polyelectrolyte complexation; iPSCs, induced pluripotent stem cells; mNSCs, mouse neural stem cells; N.A., not applicable; NaDBS, sodium dodecylbenzenesulfonate; NRCM, neonatal rat cardiomyocytes; NTE, neural tissue engineering; p123, poly(ethylene glycol)-block-poly(propylene glycol)-block-poly(ethylene glycol); PAR, polyarylate; PCL, polycaprolactone; PGS, poly(glycerol sebacate); PLA, polylactic acid; PLCL, poly(L-lactic acid-*co*-ε-caprolactone); PLGA, poly(lactic-*co*-glycolic acid); PLO, poly-ornithine; py, pyrrole; PPy, polypyrrole; PSS, polystyrenesulfonate; PT, polythiophene; p-TSA, p-toluene sulfonic acid; PVA, polyvinyl alcohol; RAECs, rat aortic endothelial cells; SA, sodium alginate; SC, Schwann cell; SF, silk fibroin.

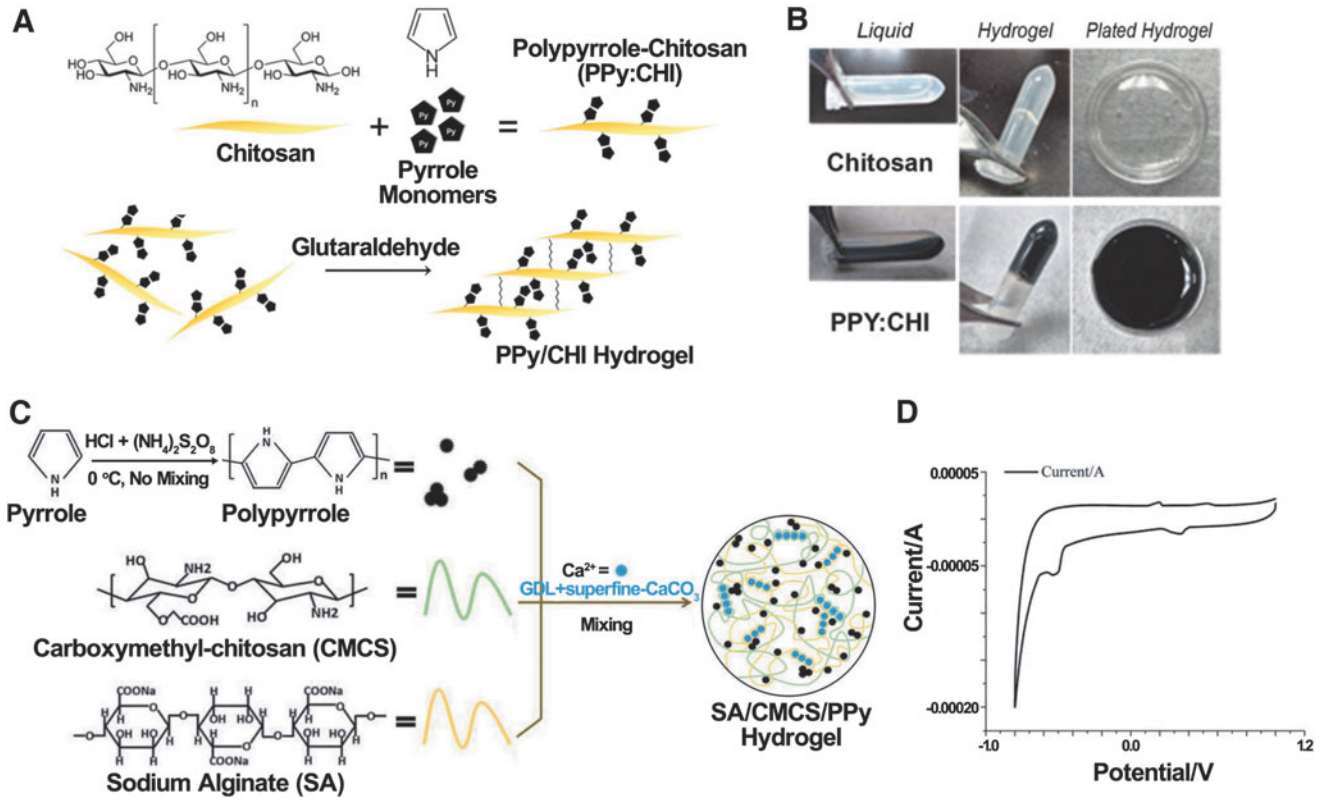

FIG. 2. **(A)** Process of CHI/PPy hydrogel generation. **(B)** CHI and CHI/PPy hydrogel coated on Petri dish. Reproduced from Cui et al.[37] with permission from Theranostics. **(C)** Fabrication of SA/CM-CHI/PPy hydrogel. **(D)** Cyclic voltammograms for the SA/CM-CHI/PPy hydrogel. Reproduced from Bu et al.[39] with permission from The Royal Society of Chemistry. CM-CHI, carboxymethyl chitosan; SA, sodium alginate.

is biocompatible, biodegradable, nontoxic, and nonimmunogenic. In the presence of divalent cations (e.g., Ca^{2+} and Ba^{2+}), ALG quickly forms ionically cross-linked networks.[41] Therefore, it can be easily processed into different formats for tissue engineering applications, such as hydrogels, microspheres, microcapsules, sponges, foams, and fibers.[42]

A conductive hydrogel based on ALG and PPy was synthesized by Yang et al. ALG hydrogel was first made and then immersed in py monomer for a completed diffusion before adding $FeCl_3$ for the polymerization (Fig. 3A, B).[43] Concentrations of the py monomer solutions ranged from 0 to 20×10^{-3} M. PPy was confirmed to be incorporated to the ALG from the FTIR results with increased intensities of C-N stretching peaks at 1220, 1260, and 1363 cm^{-1}, and a C = O stretching peak at 1716 cm^{-1} (Fig. 3C). More recently, an injectable hydrogel was made by Ketabat et al., wherein fine powder of ALG-grafted-PPy was made and then added to ALG solution, together with acid solubilized collagen (COL). Calcium chloride was used as the crosslinker to form the hydrogel.[9]

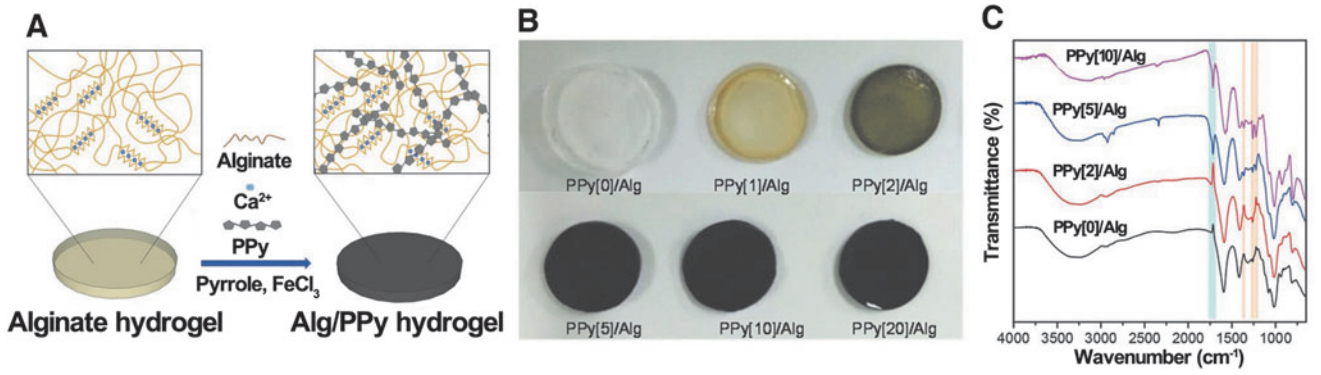

FIG. 3. **(A)** Generation of ALG and PPy/ALG hydrogel. **(B)** Various PPy/ALG hydrogels synthesized with different pyrrole monomer and oxidant concentrations. **(C)** ATR-IR spectra of PPy/ALG samples. Reproduced from Yang et al.[43] with permission from Marcomolecular Bioscience. ALG, alginate.

In addition to hydrogels, porous scaffolds based on ALG/PPy blend and CHI were also developed by Sajesh et al.[44] They conduct *in situ* polymerization to generate an ALG/PPy blend, followed by two different lyophilization steps. The first one was carried out after mixing CHI with the ALG/PPy blend. After crosslinking, another round of freeze-drying was performed. The existence and shifts of distinctive FTIR peaks of PPy and ALG confirmed the success of the blending. However, a decrease in scaffolds porosity was exhibited compared with pure CHI scaffold due to the ALG/PPy particles acting as a filler in the CHI matrix. As for *in vitro* degradation, after 28 days of immersion in PBS with lysozyme, up to 30% of the total weight of ALG/PPy/CHI scaffolds was degraded, lesser than that of the pure CHI scaffold, indicating the increased stability of the scaffold with the additional PPy.

Regarding mechanical properties, previous studies found that an increased portion of conductive polymer, PEDOT, in the composite led to a higher Young's modulus.[45] Corresponding results reported that an increased amount of PPy led to a higher Young's modulus. Compared with ALG/PPy(0), Young's modulus of PPy-containing ALG hydrogel increased by two orders of magnitude. Still, it remained less than 200 kPa for ALG/PPy(10).[43] The mechanical and structural stability were postulated to be promoted by the reaction of the positively charged PPy with anionic ALG chains.[9] However, when PPy concentration of the composite was higher than 20×10^{-3} M, the hydrogel became fragile and heterogeneous.[43]

The conductivity of the ALG/PPy composite was confirmed to be enhanced compared with pure ALG. Sajesh et al. evaluated the surface current distribution of their porous ALG/PPy scaffold by using a scanning electrochemical microscope.[44] They found that incorporating ALG/PPy into CHI increased the surface conductivity from the range of 550 to 1000 nA, which was suitable as an interactive substrate between the seeded cells and an external electric field. Both Ketabat et al. and Yang et al. reported an increase of conductivity with more PPy incorporated. An electrochemical device with a two-electrode system was used to analyze the electrical conductivity of the hydrogels in the study of Yang et al.; an increasing trend of conductivity was displayed with an increasing content of PPy, from $8.2 \pm 3.8 \times 10^{-6}$ S/cm of ALG/PPy(0) to $1.1 \pm 0.3 \times 10^{-4}$ S/cm of ALG/PPy(10).[43]

Silk fibroin. Silk is produced by silkworms and is composed of two main kinds of proteins: fibroin and sericin.[46] Silk fibroin (SF) is one of the strongest natural fibers due to its repetitive amino structure of glycine-alanine-glycine-alanine-glycine-serine in an anti-parallel β-sheet structure.[47] Due to its favorable biocompatibility and controllable degradation rates, recently SF has been increasingly studied for tissue engineering. It has been processed into different forms to serve as a scaffold for tissue engineering, including films, fibers, hydrogels, and sponges.[48]

Coating is a popular method to introduce PPy to SF. Some groups worked on coating PPy on lyophilized SF or electrospun SF scaffolds by using *in situ* polymerization. Hardy et al. immersed the freeze-dried SF in an aqueous environment with py, APS, and $FeCl_3$.[49] Distinctive peaks of amide I and amide II were found in the FTIR spectrum of PPy-SF foam, whereas peaks at 1203 cm^{-1} (S = O stretching), 927 and 895 cm^{-1} (C–H out-of-plane deformation of aromatic rings and/or bipolaron bands) demonstrated the interpenetrating network of conductive polymers. The freeze-dried SF/PPy product had similar pore size distribution, swelling ratio, and equilibrium water content as pure SF foam. However, there was a moderate reduction in porosity in SF/PPy, mainly due to the attachment of the PPy. PPy was also coated on electrospun SF mats by Aznar-Cervantes et al.[50] Thicker fibers were found on PPy-coated SF electrospun fibers, confirming the extra layer of PPy on the fiber surface. Spectrum peak for amide I in FTIR shifted to a lower wavenumber (1631 cm^{-1}) in the PPy-coated SF mat, relative to 1640 cm^{-1} in the pure SF mat, inferring an increase of the crystallinity in the mats (understood as a higher β-sheet content). Another group coated PPy on a 3D-printed SF scaffold, followed by electrospinning another thin layer of SF on the composite to enhance the attachment of PPy and provide fibers of nanostructure for cell growth.[1]

Functionalization of several amino acids on the SF's backbone has been demonstrated to make SF more reactive.[51] Hence, acid-modified SF was used to allow a better incorporation of PPy. Some groups used diazonium coupling, wherein tyrosine side chains of insoluble SF film were reacted with sulfanilic acid and p-toluene sulfonic acid (p-TSA) in borate buffer (Fig. 4A, D).[51–53] The acid-modified SF film was then submerged in the monomer-oxidant solution for polymerization (Fig. 4B, D). After acid modification, it was easier for the positively charged PPy to get incorporated into the negatively charged silk network. Further, this method significantly reduced the amount of py and $FeCl_3$ needed for polymerization compared with using unmodified silk.[50]

Mechanical property changes of adding PPy to SF scaffolds in different formats were compared. For lyophilized products, there was a slight drop in SF/PPy foam compared with SF foam. The compressive modulus and strengths were 74.7, 7.4 kPa for PPy/SF foam, and 99.3, 9.2 kPa for SF foam, respectively.[49] Both the PPy-coated electrospun SF mat and PPy-coated acid-modified SF film presented an increase in Young's modulus.[50,51] Aznar-Cervantes et al. found that the mechanical resistance of SF/PPy mat increased to support a breaking force higher than 5 N and an extension more than 0.3 mm after coating, relative to the pure SF (2–3 N, 0.12–015 mm).[50]

As for the conductivity of the scaffold, the shape of the voltammograms of the PPy-coated electrospun SF mesh reported by Aznar-Cervantes et al. was similar to those previously reported for free-standing PPy and PPy-coated Pt electrodes in aqueous solutions, indicating that the SF/PPy mesh could support the flow of a broad range of anodic and cathodic currents in the cell proliferation bath.[54,55] An enhancement of conductivity after incorporating SF film with PPy was also reported by Tsui et al.[52] The addition of PPy significantly reduced substrate resistivity from values greater than 10^6 Ω/sq of acid-modified SF substrate to the range of 200–500 Ω/sq. The result was further illustrated by the I–V curve (Fig. 4E), where the acid-modified substrate showed no response to the applied voltage, whereas the PPy-coated substrate displayed a nonlinear curve.

For degradation studies, Zhao et al. incubated the composite scaffold, a PPy-coated 3D-printed SF substrate with electrospun SF fibers covered on top, in water and Dulbecco's modified Eagle's medium for 30 days.[1] They observed a

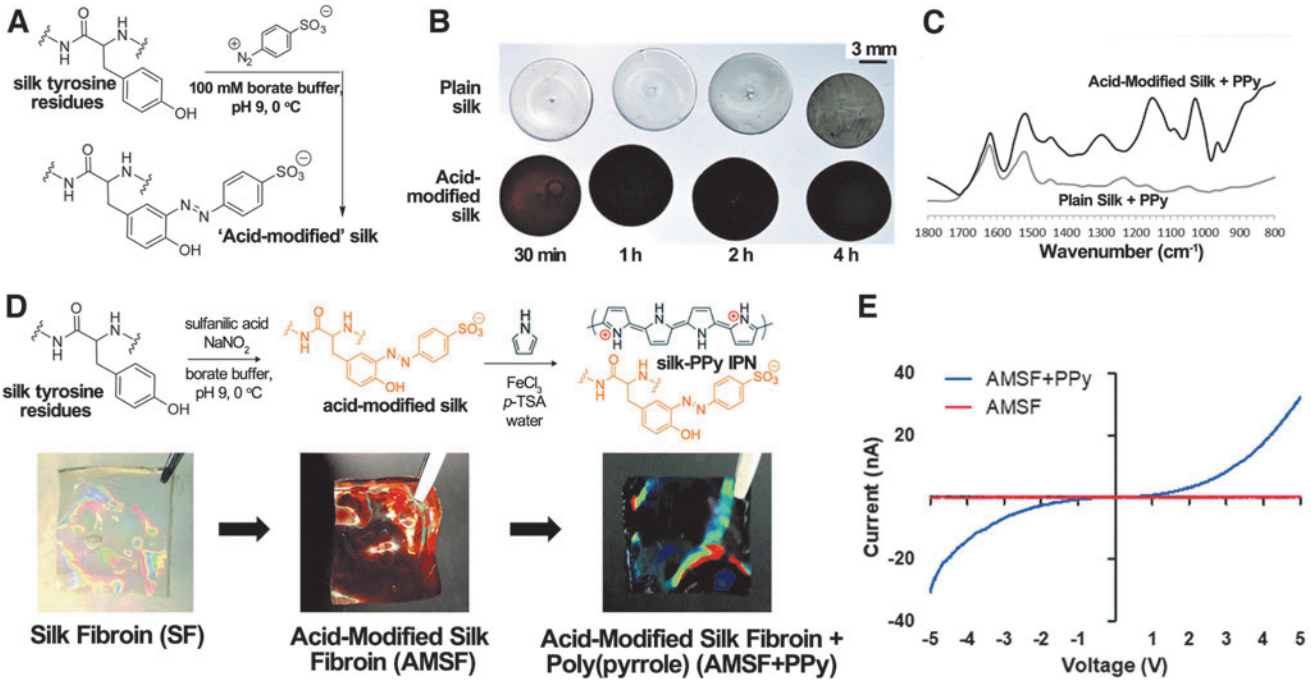

FIG. 4. **(A)** Diazonium coupling reaction used to synthesize AMSF. **(B)** SF and AMSF films exposed to 50 mM pyrrole and 7.5 mM $FeCl_3$ in water for the times given. **(C)** ATR-FTIR spectra of SF and AMSF after Ppy deposition for 2 h. Reproduced from Romero et al.[51] with permission from ACS Applied Materials and Interfaces. **(D)** Fabrication of AMSF and AMSF/PPy. **(E)** I–V curves of AMSF and AMSF/PPy substrates. Reproduced from Tsui et al.[52] with permission from The Royal Society of Chemistry. AMSF, acid-modified silk fibroin; FTIR, Fourier Transform Infrared; SF, silk fibroin.

more significant loss of mass for the construct without the extra layer of electrospun SF fibers. PPy-coated acid-modified SF films were exposed to solutions containing a high concentration of protease XIV, which is the commonly used enzyme to mimic silk degradation *in vivo*, to accelerate the degradation process in the study by Romero et al.[56–58] It showed that acid-modified SF film degraded faster than the unmodified one, mainly due to the increase in hydrophilicity. Films with PPy coatings only had an 8% mass loss after 10 days, lower than the uncoated one, which was postulated to be due to the protection from the PPy coatings.[51] A consistent result of a slower mass loss profile of PPy-containing SF lyophilized foam relative to SF foam was observed by Hardy et al., reportedly due to the interpenetrating network of the PPy prohibiting the enzyme from getting close to the backbone of the protein.[49]

Other natural materials. Other natural saccharide materials, such as hyaluronic acid (HA) and xanthan gum (XG), were fabricated into conductive hydrogels with PPy. Yang et al. used the covalent bond formation between HA and py to enhance structural stability and uniformity of hydrogel. Py-conjugated HA hydrogel was created and then polymerized by using APS. The color of the hydrogel became darker with more py monomer and oxidant used, reflecting the amount of the PPy formed inside the hydrogel. Both conductivity and modulus of the hydrogels increased till the py concentration in the polymerizing solution reached 50 mM.[59] HA and gelatin were also fabricated into conductive adhesive hydrogel with dopamine-modified PPy by Wu et al.[60] Polysaccharide such as XG hydrogel was incorporated with PPy through electropolymerization.[61] Enhanced electrical conductivity compared with pure XG hydrogel was confirmed by cyclic voltammetry evaluation, where PPy/XG hydrogel exhibited similar redox peaks as PPy. Proteins such as COL were also mixed with PPy as a fibrous scaffold by using the method of interfacial polyelectrolyte complexation (IPC).[62] An inclusion complex made of py and 2-hydroxypropyl-β-cyclodextrin underwent the process of IPC with cationic methylated COL to achieve py-incorporated COL fibers. $FeCl_3$ was then used to initiate the polymerization. Hybrid microfibers hydrogel was developed via mixing synthesized PPy with COL according to Wu et al.[63]

Conjugation with synthetic materials

Polycaprolactone. Polycaprolactone (PCL) is an FDA-approved synthetic biodegradable polyester. It is semi-crystalline with a low melting point of 60°C and good ductile and elastic properties.[13] It also has exceptional mechanical properties and a lower fabrication cost based on the ease of synthesis. PCL has been combined with PPy in different ways to fabricate conductive scaffolds for tissue engineering applications.

Spearman et al. fabricated PCL films with PPy coatings by conducting a 24-h *in situ* polymerization.[10] A shift of the nitrogen 1 s peak from X-ray photoelectron spectroscopy results confirmed the successful polymerization of PPy on the PCL backbone. PCL scaffolds with nanoscale fibers were also obtained by using electrospinning.[13,64] Kai et al. added doped PPy together with PCL/gelatin (PG) to the organic solvent HFP to form the spinning solution.[13] PPy-related

FTIR peaks, including N-H stretching band at 3400 cm^{-1}, symmetric C = C ring at 3100 cm^{-1}, and C-H deformation in py ring, were found in the composite. On the other hand, Hardy et al. generated an interpenetrating network of PPy on electrospun PCL nonwoven mat by *in situ* polymerization.[64] Compared with the X-ray photoelectron spectra of PCL with no peaks, a peak appeared at 400 eV in that of the PCL/PPy fibers, implying the incorporation of PPy. Products using *in situ* polymerization usually result in the entire scaffold coated with PPy coatings, so Shafei et al. used the method of vapor phase polymerization to coat PPy only on the scaffold surface.[65] PCL mats were first obtained by electrospinning; then, the oxidant, ferric p-toluene sulfonate, was electrosprayed onto the electrospun PCL mat. It was followed by putting the mats in a closed chamber containing py for an hour until the surface of the mats turned black. Some groups focus on having a more precise control of the scaffold's fiber diameter and pore size, wherein a method such as electrohydrodynamic jet 3D printing was explored.[66]

Spearman et al. showed that the hardness and elastic modulus of PCL films were statistically similar before (0.073 ± 0.008, 1.07 ± 0.05 GPa) and after coating with PPy (0.071 ± 0.02, 0.93 ± 0.19 GPa).[10] Similar results were also observed from Hardy et al., wherein there were no significant differences in yield strength and ultimate tensile strength between PCL electrospun meshes, with and without PPy coatings, but a slightly smaller value was observed for the one with PPy coatings.[64] In contrast to the results from the studies just cited, Kai et al. reported that the Young's modulus of PPy/PG electrospun mats increased with PPy content, from 7.9 ± 1.6 MPa for PG fibers to 50.3 ± 3.3 MPa for PPG30 fibers, which could be due to the addition of gelatin in the composite as well as the form of the composite. Meanwhile, the maximum elongation of the nanofibers dropped dramatically from $61.1\% \pm 17.3\%$ for PG fibers to $3.7\% \pm 1.4\%$ for PPG30 fibers.[13]

As for conductivity, the nonconductive NaOH-treated PCL films, which possess infinite resistivity, were improved by the interpenetrating network of PPy, with an average resistivity of 1.0 ± 0.4 k$\Omega \cdot$cm.[10] In the study of Kai et al., conductivity profiles of PPy/PG:15:85 (PPG15) and PPy/PG:30:70 (PPG30) electrospun mats were compared.[13] There were linear variations of current with voltage in both I–V profiles, implying that the PPy-containing scaffolds were conductive. Moreover, there was a trend of higher electrical conductivity with a higher concentration of PPy in the composite, based on the results that conductivities increased from 0.013 mS/cm for PPG15 to 0.37 mS/cm for PPG30. Shafei et al. found that electrospraying oxidants on the surface of PCL mats for only 0.5 h was not enough to achieve a conductive scaffold.[65] Meshes that have been electrosprayed for 1–4 h became conductive, with surface resistivities ranging from 3.6–21.2 kΩ/sq, which was reported to be much lower than using traditional solution-dipping *in situ* polymerization.

For degradation studies, a slower degradation rate was found in PCL scaffolds containing less PPy. Degradation behavior was evaluated by Kai et al. by immersing the nanofibers in PBS for 8 days.[13] Scaffold morphology was observed with scanning electron microscopy. Results showed that all the samples had a certain degree of swelling and degradation, but an apparent morphological change was observed in the scaffold with the highest PPy content (PPG30). They concluded that regardless of the excellent conductivity and better mechanical properties with higher PPy content, this rapid degradation would probably result in immediate loss of electrical conductivity and mechanical properties, which is not suitable for long-term implants in tissue engineering.

Other synthetic materials. Other synthetic materials, such as poly(L-lactic acid-*co*-ε-caprolactone) (PLCL), poly(lactic-*co*-glycolic acid) (PLGA), and polyarylate, were used to incorporate with PPy as a conductive substrate. Sun et al. used *in situ* polymerization to coat PPy on electrospun SF/PLCL scaffolds.[6] Increased roughness of the electrospun fibers was due to the deposition of PPy on the fiber surface. Both surface resistance and water contact angle dropped with increasing amounts of py monomer, and oxidant was added. In terms of mechanical properties, Young's modulus of the PPy-coated PLCL/SF membranes was significantly higher than that of PLCL/SF. On the other hand, electrospun PLGA mats were fabricated by Gelmi et al. and Lee et al. with different methods to integrate PPy.[67,68] Gelmi et al. performed a two-time polymerization, namely py vapor and electrochemical polymerization, whereas Lee et al. simply conducted an *in situ* polymerization by immersing the mat into py monomers and an oxidant. PPy was also freeze-dried with synthetic hydroxyapatite as a potential scaffold for bone tissue engineering according to Zanjanizadeh et al.[69] They reported that PPy did not alter the compressive mechanical properties as much compared with the scaffold made of hydroxyapatite only. In another study conducted by Weng et al., inkjet-printable PPy ink was made and printed onto a polyarylate film. Subsequently, COL was printed on top of the PPy. Only conductivity of the printed PPy lines was provided, which was 1.1 S/cm. Atomic force microscopy results showed a decrease in surface roughness of the scaffold from 8.86 to 4.45 nm after adding the additional layer of COL to the PPy lines.[70]

To summarize, PPy has been integrated with multiple materials as scaffolds for tissue engineering (Table 1). *In situ* polymerization was the most common method, wherein oxidant, mainly $FeCl_3$ and APS, and dopant, commonly NaCl and p-TSA, were added to the py monomer aqueous solution. PH of the polymerization system is adjustable based on the requirement of the base material. Some studies fabricated the main part of the scaffold first and then coated PPy on the substrate, which is referred to as immerse coating in this review. To ensure better polymerization, substrates were usually presoaked in py monomer, which allows a full monomer infusion before adding the oxidant to initiate *in situ* polymerization. Some other groups mixed py monomer with the base material before scaffold fabrication to create some possible covalent bonds. Meanwhile, some studies used commercialized doped PPy instead of *in situ* polymerization to avoid inconsistency of the conductivity of the final product. However, variations of dopants, temperature, length of polymerization, and stirring affect the conductivity of PPy.[12,26] The base material of the scaffold provided mechanical properties to reduce the brittleness of the PPy, whereas the addition of PPy provided the electrical conductivity of the insulating base materials. Most studies showed higher conductivity of the composite with increasing PPy content. However, this led to a proportional compromise of mechanical properties. Therefore, the amount of PPy and the fabrication method

should be optimized based on the application of the scaffolds. Biocompatibility and potential utility of these PPy-containing scaffolds in tissue engineering will be discussed in the next section.

Applications in Tissue Engineering

Since nerve, bone, muscle, and cardiac cells respond to electrical impulses,[9] several studies have employed the use of conductive scaffolds containing PPy to regenerate these tissues. Cells possess identical bioelectric properties, which controls cell functions based on cellular membrane potential.[71,72] On the membrane of these electrically excitable cells, voltage-gated Ca^{2+} channels (VGCCs) play a critical role in the electrical current generation.[71] It controls intracellular Ca^{2+} concentration and, hence, initiates electrical function in the regenerative process, such as genes and proteins expression, differentiation, and maturation.[73,74] The principal idea of using electrically conductive PPy-containing scaffolds is that they would be better suited to provide electrophysiologically representative support and modulate the ion flux and VGCC's activity. In this section, we will discuss the outcomes of using PPy-containing scaffolds in tissue engineering.

Nerve tissue engineering

The rate of morbidity is high among patients suffering from nerve damage caused by a neurological condition or trauma.[75,76] The treatment modalities for these include autografting, allografting, and xenografting. Autografting comes with the morbidity issues in the donor site, whereas allografting and xenografting might cause serious immune rejection.[76] This elucidates the motivation for fabricating feasible synthetic nerve grafts through tissue engineering. Generally, scaffolds for nerve cells should possess the appropriate hierarchical structure, chemical and topographical properties. However, recent studies reported that adequate electrical stimulation could potentially induce nerve cell differentiation and promote axonal growth of neurons, which seems to allude to the possible benefits of conductive nerve graft scaffolds.[39] To this end, several investigations have been conducted on using electroconductive materials to guide and promote nerve reconstruction and neurogenesis. The potential use of conductive polymers in nerve tissue engineering was first found in the study by Schmidt et al., where PC12 cells grown on PPy films demonstrated an enhanced neurite outgrowth with electrical stimulation.[77] Since then, conductive scaffolds using PPy and other conductive polymers were explored in nerve applications. For example, the 3D-printed conductive PPy/PCL scaffold was rolled to a tubular conduit for peripheral nerve repair.[66] The PLGA/PPy scaffold with a microgroove layer was used in neural stem cell differentiation.[78]

Cell adhesion, distribution, and viability have also been investigated to evaluate the biocompatibility of PPy-containing scaffolds. In one such investigation, composite scaffolds of ALG/PPy hydrogel were shown to have a significantly better cell adhesion as compared with scaffolds of pure ALG, which lacks cell-binding moieties and is known to have poor protein adsorption and cell adhesion.[43] Moreover, functional conductive hydrogels made of SA, CM-CHI, and PPy were found to support the proliferation of PC12 cells. They guided a more uniform cell distribution when compared with scaffolds without PPy. The authors reasoned that the improved uniformity was due to the extra cell support conferred by the PPy particles.[39] However, not all findings support this hypothesis. In a study by Weng et al., no significant differences in PC12 cell adhesion and viability were found between PPy-coated and -noncoated PLGA electrospun scaffolds.[70] In addition, Tian et al. reported, contrastingly, that the addition of PPy had a negative effect on PC12 attachment. Aligned polylactic acid (PLA) electrospun fibers without PPy were found to have better cell attachment and showed a higher cell proliferation rate.[4] However, it should be noted that the differences in base materials and formats of the scaffolds would also affect cell growth. Further, cell alignment, neurite outgrowth, and length were found to be influenced by fiber alignment rather than the deposition of PPy.[5,70]

The effects of PPy-containing scaffolds on cell differentiation, without an external electrical stimulation, were explored by Yang et al.[43] Human mesenchymal stem cells (hMSCs) were seeded to the hydrogels and incubated in a neural differentiation media. Expressions of Tuj1 and MAP2, early and late neurogenesis markers, were compared between hMSCs cultured on tissue culture plate and those cultured on ALG/PPy hydrogel. RT-PCR results reflected an upregulation of this nerve-specific gene expression on the conductive hydrogel, with a notably 10-fold increase in MAP2 at d14 compared with d7. However, the exact reason for this remarkable enhancement requires further investigation. Aside from the conductive substrates, other factors, such as material property and protein adsorption, could also have been contributing to the observed improvement in the neural differentiation. Other supportive findings reported that a conductive PCL/PPy scaffold enhanced human embryonic stem cell-derived neural crest stem cells maturation toward peripheral neuronal cells,[66] and PPy/COL hydrogel microfibers improved neurogenesis of PC12 cells.[63]

Though without electrical stimulation, conductive scaffolds affect neuronal differentiation. Many groups reported that additional electrical stimulation has a strong influence on cell growth and differentiation.[77,78] Bu et al. reported that, together with electrical stimulation, PPy-containing hydrogels were able to promote axon development in RSC96 cells.[39] They reasoned that PPy allowed for good material exchange and provided metabolic sites for the cells. In a related study by Lee et al., PPy-containing electrospun PLGA scaffolds were subjected to electrical stimulation to determine whether conductive nanofibers could deliver electrical signals.[68] They reported a significantly higher amount of neurite-bearing PC12 cells and longer neurites in the groups with electrical stimulation compared with the unstimulated controls (Fig. 5B, C).

Some studies directly compared the effects of electrical stimulation on both scaffolds with and without PPy, which helps to elucidate the role of conductive materials in the scaffold. Sun et al. demonstrated better cell proliferation rate of Schwann cells (SCs) on the electrospun PLCL/SF scaffold with PPy coatings, relative to the pure PLCL/SF scaffold (Fig. 5A).[6] They also found a further increase in cell population on the PLCL/SF/PPy scaffold with an electrical stimulation. Differentiation of PC12 cells was done without adding nerve growth factor. Interestingly, no differentiated

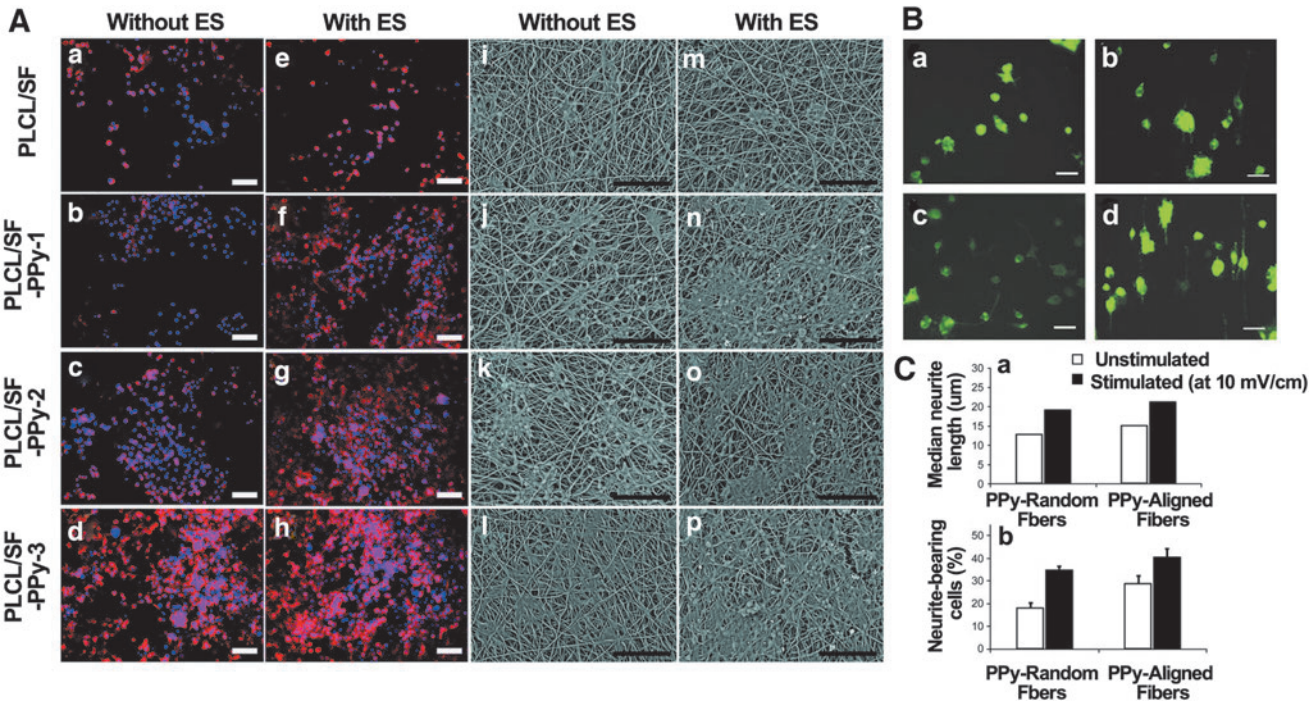

FIG. 5. **(A)** Fluorescence images of SCs cultured on different nanofiber membranes without ES **(a–d)** and with ES **(e–h)**; SEM images of SCs cultured on different nanofiber membranes without ES **(i–l)** and with ES **(m–p)**. PLCL/SF-PPy-1, -2, -3 represent different Py concentrations, from 25, 37.5, 50 μL, respectively. Scale bars are 100 mm. Reproduced from Sun et al.[6] with permission from The Royal Society of Chemistry. **(B)** Fluorescence images of electrically stimulated PC12 cells on PPy/PLGA scaffolds with random fibers at 0 mV/cm **(a)**; at 10 mV/cm **(b)**; with aligned fibers at 0 mV/cm **(c)**; at 10 mV/cm **(d)**. Scale bars are 50 μm. **(C)** Median neurite lengths **(a)** and percentages of neurite-bearing PC12 cells **(b)** with or without electrically stimulated. Reproduced from Lee et al.[68] with permission from Biomaterials. PLCL, poly(L-lactic acid-*co*-ε-caprolactone); PLGA, poly(lactic-*co*-glycolic acid); SC, Schwann cell; SEM, scanning electron microscopy.

PC12 cells were found on PPy-containing scaffolds in the absence of electrical stimulation. Under electrical stimulation, differentiated PC12 cells were observed on the nonconductive scaffold, but in a much smaller proportion than that found on the conductive scaffolds. Therefore, the authors concluded that the electrical stimulation can induce PC12 differentiation, whereas the conductive property of the substrate can only enhance but not induce the differentiation. Wu et al. investigated the mechanism of elevated neurogenesis by conductive materials and electrical stimulation by comparing the intracellular Ca^{2+} concentration.[52] They reported an increment of approximately twofold in the PPy-containing group, whereas a further increase was noticed after applying electrical stimulation. An increased fold of Ca^{2+} level after stimulation was larger in the PPy-containing group than the control group. These results were explained by the upregulated expression of VGCCs from the conductive matrix and electrical stimulation. Hence, elevated Ca^{2+} influx regulated neurogenesis-related gene expression. Moreover, *in vivo* studies were carried out and PLA/PPy scaffolds could inhibit scar tissue formation and induce the axonal regeneration.[79,80]

Bone tissue engineering

Aimed at providing a new approach to treat bone conditions and disorders, especially the common clinical problem of bone defects, bone tissue engineering was introduced to replace the conventional methods that often require additional surgeries.[81,82] To facilitate bone tissue regeneration, the principal strategy of bone tissue engineering is to proliferate osteogenic cells in a porous and osteoconductive 3D scaffold together with inductive growth factors. Since osteocytes are responsive to external electric fields,[83] conductive biomaterials have been exploited for fabricating scaffolds to fulfill the electrophysiological requirements for bone development. Preliminary studies by Langer R group utilized a 2D PPy film to investigate osteogenic differentiation of bone marrow-derived stromal cells.[11] Subsequently, the potential of PPy-containing electroactive scaffolds for bone tissue engineering has been explored by various other research groups.

It is imperative for materials used in bone tissue engineering to have comparable mechanical properties to those of native bones. Zanjanizadeh et al. created a mesoporous silica PPy-based scaffold with similar mechanical strength (7 MPa) and Young's modulus (0.11 Gpa) as a cancellous bone,[69] which has a compressive strength around 2–12 MPa and a Young's modulus of 0.05–0.5 GPa.[84]

PPy-containing scaffolds were found to enhance cell proliferation according to Pelto et al. Cell numbers after 14 days of culturing were compared between PLA and PLA/PPy scaffolds, with and without electrical stimulation during the culture.[85] A higher cell number was observed on the PPy-coated scaffold, whereas electrical stimulation did not have any effects on cell proliferation. However, in another study, lower deoxyribonucleic acid content was measured from the

PPy-containing PCL electrospun scaffold, seeded with hMSCs, as opposed to a pure PCL scaffold.[64] This was primarily due to the weak cell adhesion that commonly occurs on matrices containing conductive materials, which usually need to be modified with cell adhesive moieties. On the other hand, enhanced alkaline phosphatase (ALP) activity and Ca^{2+} deposition were observed on the electrospun PCL mat with an interpenetrating network of PPy, contributing to the variation of protein deposition on the scaffold.

Changes in surface chemistry and roughness of the scaffold by adding PPy could alter protein deposition from the medium onto the scaffolds, hence affecting cell differentiation. Therefore, thick porous scaffolds made of SF with PPy coatings were fabricated by Hardy et al. to enhance osteogenic differentiation of hMSCs.[49] They concluded that a nonconductive silk scaffold supported hMSCs differentiating toward osteocytes, whereas the addition of an electrical stimulus together with a PPy-coated conductive scaffold enhanced osteogenic differentiation, which was determined by the increased ALP expression, calcium deposition, and COL production. No differentiation medium or growth factors were involved in the osteogenic differentiation study of human adipose-derived stem cells conducted by Pelto et al.,[85] However, osteogenic differentiation was found to improve with cells cultured on PPy-coated PLA scaffolds, relative to those on pure PLA scaffolds. However, they did not find significant differences in early osteogenic differentiation (d1, d7, d14) or proliferation between the electrically stimulated and nonstimulated groups, contrary to other studies.

Cardiac tissue engineering

The leading cause of heart failure is myocardial infarction.[86] This impairment is irreversible and permanent due to the heart's limited ability to regenerate cardiomyocytes (CMs). To further exacerbate the issue, the resulting inflexible and fibrous scar tissues delay the impulse conduction within the heart. It restricts the contractile function of the left ventricle and eventually results in an asynchronous contraction, increasing the possibility of congestive heart failure.[87,88] Therefore, patches made of various biomaterials, mimicking the ECM of CMs, have been investigated as a means to stabilize the infarcted region. However, rebuilding a similar architecture to the native ECM is insufficient, since maintaining the electrophysiological conductivity is vital in restoring the functionality of the myocardium. Given that most of the current scaffolds are made of insulating materials, which cannot support electrical propagation, there is a need to develop electrically conductive scaffolds to restore the synchronicity of cardiac contraction.

Enhanced CM's adhesion and proliferation on conductive PPy-containing electrospun mat was reported by Kai et al.[13] Though the exact mechanism is yet unclear, assumptions include electrostatic effects and protein adsorption. Since PPy is positively charged, though the cell membrane is negatively charged, CM's attachment could be strengthened by the electrostatic force. Meanwhile, PPy alters the local electrostatic charge of the scaffold, resulting in an alteration in protein adsorption of the scaffold, which further enhances cell attachment based on cell–material interaction *in vitro*.[13,89]

Calcium transient plays a vital role in regulating the CM's function. Average calcium transient wave velocity across the HL-1 cell was found to be much higher on PCL/PPy film (1612 ± 143 μm/s) than that on PCL film (1129 ± 247 μm/s).[10] Similarly, He et al. reported an enhanced Ca^{2+} signal conduction of neonatal rat CMs when the CHI/PPy gel patch was used.[38] The improvement in transient velocity observed was postulated due to (1) transient activity of specific channel currents and (2) external electrical or mechanical changing cell–cell coupling.[10] Another study conducted by Cui et al. demonstrated CHI/PPy hydrogel's ability to improve the synchronization of the isolated CM's population.[37] They designed a unique culture model to investigate whether the electrical signals generated by CMs, cultured on a conductive biomaterial, can synchronize with neighboring CMs, without external stimulation (Fig. 6). CMs were cultured in the center, or the peripheral area of a CHI- or CHI/PPy-coated culture plate. There was no direct connection between the CMs in these two areas. By evaluating Ca^{2+} transients, they determined that the contraction of these physically isolated CMs could, indeed, be synchronized by CHI/PPy hydrogel without an external stimulation. In addition, they observed no synchronization on cells cultured on CHI-coated or -noncoated plates.

Sarcomeric α actinin (Sar), Connexin 43 (Cx43), and Troponin T (TnT) are critical cardiac-specific proteins involved in CM's contraction. Tsui et al. demonstrated, through immunostaining, a remarkable improvement in both the sarcomere length and expression of Cx43 of the human pluripotent stem cells (PSCs)-derived CMs on PPy-containing acid-modified SF film.[52] However, no obvious impacts on CMs were found between PPy-coated and -uncoated scaffolds, for the Z-band width of sarcomere and Cx43 polarization and distribution. Instead, they were shown to be influenced by the topography of the scaffold. In a study by Kai et al., the expressions of Sar and TnT were found to be high in both PCL/gelatin scaffolds with and without PPy.[13] Still, a remarkably higher density of Cx43 was found on the PPy-containing electrospun PLGA mat. In contrast, Spearman et al. found no significant differences of Cx43 gene expression, through PCR quantification, between HL1 cultured on PPy-coated and -uncoated PCL film, aside from a change in intracellular location.[10] Although the effects of PPy on cardiac-specific protein expression seem to demonstrate only minor differences in the studies cited earlier, they all found that PPy had the potential to alter the expression of these proteins. It has been hypothesized that the conductive PPy scaffold surface can induce hyperpolarization of the CM's membrane potential, accelerating their maturation[52,90]

External electrical stimulation was previously found to be able to direct the growth and adjust electrophysiological properties of CMs, in both monolayers and cells-seeded conductive scaffolds containing gold nanowire,[7] gold nanoparticles,[91] and carbon nanotubes.[8,92,93] Most electrical stimulation assessments involving PPy were done on tissues. For example, *ex vivo* assessment of the conduction velocity after 28 days of implanting patches on a scar tissue was done by Cui et al.[37] A higher electromyography signal amplitude was observed in CHI/PPy-treated myocardial scar tissues. On the other hand, the effects of electrical stimulation on cardiogenetic differentiation, explored by another group, noted that induced PSCs seeded on PLGA/PPy had an elevated expression of Sar, as compared with the PLGA control.[67]

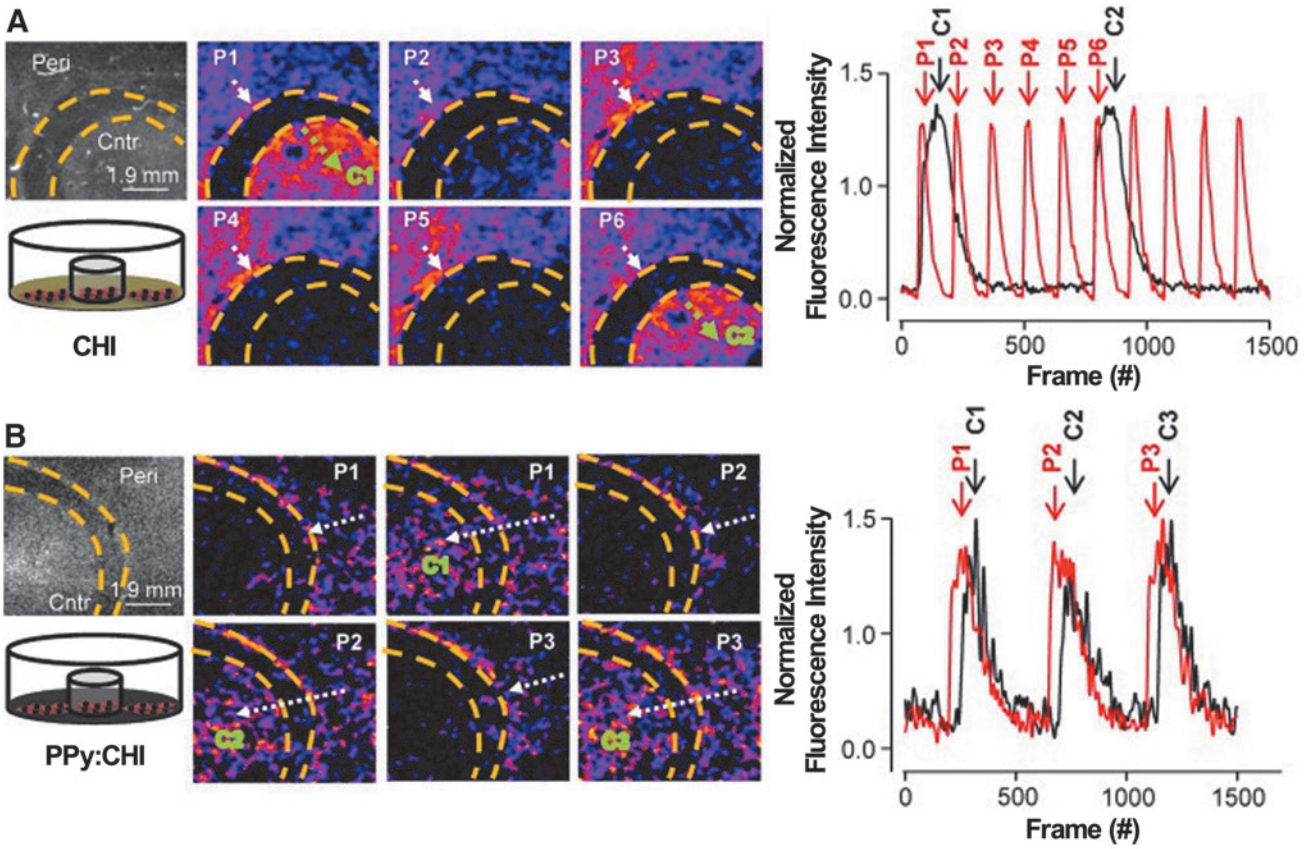

FIG. 6. Calcium transients and normalized fluorescence intensity against time for CMs on **(A)** CHI-coated Petri dish, **(B)** PPy/CHI-coated Petri dish. Reproduced from Cui et al.[37] with permission from Theranostics. CMs, cardiomyocytes.

Patches have also been implanted onto rat hearts for *in vivo* studies. Implantation of the CHI/PPy gel patch (without cells) not only had no alterations on the native electrical signal propagation but also improved conduction velocity in defect areas.[38] This result supports the findings by Cui et al., who reported similar longitudinal conduction velocities, measured by optical mapping, in both CHI/PPy-treated heart (81.3 ± 0.59 cm/s) and the uninjured controls (74.3 ± 4.7 cm/s), after 28 days of implantation.[37] To avoid suturing, the conductive adhesive hydrogel was developed. It was confirmed to be able to adhere to porcine myocardium and decreased infarct sizes.[60] Corresponding results of reducing ventricle infarction size were also reported by using the PPy/PGA spring.[94]

In summary, PPy-containing composites have been utilized in regenerating different electroactive tissues. Being biocompatible, they support cell attachment, proliferation, and growth. By using these scaffolds, both the axonal growth of neurons and the expression of neurogenesis markers were improved in nerve regeneration. In addition, enhanced ALP activity and effects on osteogenic differentiation were reported in bone tissue engineering. Further, there was a higher calcium transient wave velocity when used in regenerating cardiac tissues. Conductive PPy-containing scaffolds, external electrical stimulation, and controlled topography have synergistic influences on cell morphology, organization, and differentiation.

Conclusion

This review focuses on the recent progress of PPy-containing scaffold-based strategies used in tissue engineering. Electrospinning, freeze-drying, crosslinking, casting, and 3D printing were used to fabricate the conductive scaffold of different formats. Incorporating PPy with different polymers as a composite solves the shortcomings of using PPy alone. Brittleness of PPy was enhanced by integrating with a material with better mechanical properties. Electrical conductivity was introduced to the base material through the addition of PPy. Although the mechanical properties range widely, it is controllable by adjusting the format and materials ratio in the scaffolds, to be within a suitable range for generating different tissues.

The biocompatibility of the PPy-containing scaffolds was demonstrated by seeding different cell sources on the scaffolds and observing proper cell attachment and proliferation. The use of PPy-containing scaffolds, together with electrical stimulation, showed positive effects on cell behaviors. Hence, it is proven that using conductive PPy-containing scaffolds could be a promising strategy in tissue engineering, especially for electroactive tissues. However, the exact mechanism of how conductive material or external electrical stimulation promotes cell maturation and differentiation is yet to be elucidated. Several hypotheses are stated in previous sections, including hyperpolarization of cell membrane

resting potential, electrostatic effects, VGCC's expression and activity, and material–cell interaction. Besides, cell behaviors are regulated by many other factors in ECM: biochemical cues such as growth factors, hormones, and small chemicals; physical cues such as scaffold porosity, stiffness, and topography. Therefore, it would be beneficial for future works to focus on introducing these cues to PPy-containing materials.

Biodegradability of the scaffolds is a crucial criterion in tissue engineering. The substrate is usually intended as a temporary support to guide the cells in forming tissues. However, more studies on degradation, both *in vitro* and *in vivo,* are needed to clarify the biological fate of the PPy particles in terms of the erosion rate, assimilation, or excretion pathway. PPy-containing conductive materials are still promising for tissue engineering applications since surface modification could easily be employed to ensure the strong adherence of PPy with the base material. In addition, very little PPy is required to achieve the desired conductivity—due to its excellent intrinsic property. The amount of PPy utilized could also be controlled by using varied polymerization and fabrication methods, further justifying its use.

With more future studies to surmount the remaining concerns and optimize the PPy-containing conductive composite, these scaffolds will likely expand the available strategies in tissue engineering and possibly fulfill the unmet clinical needs.

Authorship Confirmation Statement

Y.L. wrote the article. Prof. J.C.-H.G. reviewed and gave final approval for publication. All authors have seen and approved the submission of this article to *Bioelecricity* special issue Electrically Charged Biomaterials for Drug Delivery and Tissue Repair. The authors confirm that this article has not been published previously or considered by any journal and is not under consideration for publication in any other journal.

Author Disclosure Statement

No competing financial interests exist.

Funding Information

No funding was received for this article.

References

1. Zhao YH, Niu CM, Shi JQ, et al. Novel conductive polypyrrole/silk fibroin scaffold for neural tissue repair. Neural Regen Res 2018;13:1455–1464. DOI: 10.4103/1673-5374.235303
2. Gajendiran M, Choi J, Kim SJ, et al. Conductive biomaterials for tissue engineering applications. J Ind Eng Chem 2017;51:12–26. DOI: 10.1016/j.jiec.2017.02.031
3. Tayalia P, Mooney DJ. Controlled growth factor delivery for tissue engineering. Adv Mater 2009;21:3269–3285. DOI: 10.1002/adma.200900241
4. Tian L, Prabhakaran MP, Hu J, et al. Synergistic effect of topography, surface chemistry and conductivity of the electrospun nanofibrous scaffold on cellular response of PC12 cells. Colloids Surfaces B Biointerfaces 2016;145:420–429. DOI: 10.1016/j.colsurfb.2016.05.032
5. Hardy JG, Lee JY, Schmidt CE. Biomimetic conducting polymer-based tissue scaffolds. Curr Opin Biotechnol 2013;24:847–854. DOI: 10.1016/J.COPBIO.2013.03.011
6. Sun B, Wu T, Wang J, et al. Polypyrrole-coated poly(l-lactic acid-co-ε-caprolactone)/silk fibroin nanofibrous membranes promoting neural cell proliferation and differentiation with electrical stimulation. J Mater Chem B 2016;4:6670–6679. DOI: 10.1039/c6tb01710j
7. Dvir T, Timko BP, Brigham MD, et al. Nanowired three-dimensional cardiac patches. Nat Nanotechnol 2011;6:720–725. DOI: 10.1038/nnano.2011.160
8. Shin SR, Jung SM, Zalabany M, et al. Carbon-nanotube-embedded hydrogel sheets for engineering cardiac constructs and bioactuators. ACS Nano 2013;7:2369–2380. DOI: 10.1021/nn305559j
9. Ketabat F, Karkhaneh A, Aghdam RM. Injectable conductive collagen/alginate/polypyrrole hydrogels as a biocompatible system for biomedical applications. J Biomater Sci Polym Ed 2017;28:794–805. DOI: 10.1080/09205063.2017.1302314
10. Spearman BS, Hodge AJ, Porter JL, et al. Conductive interpenetrating networks of polypyrrole and polycaprolactone encourage electrophysiological development of cardiac cells. Acta Biomater 2015;28:109–120. DOI: 10.1016/j.actbio.2015.09.025
11. Shastri VP, Rahman N, Martin I, et al. Application of conductive polymers in bone regeneration. MRS Proc 1998;550:215. DOI: 10.1557/PROC-550-215
12. Vernitskaya TV, Efimov ON. Polypyrrole: A conducting polymer; its synthesis, properties and applications. Russ Chem Rev 1997;66:443–457. DOI: 10.1070/RC1997v066n05ABEH000261
13. Kai D, Prabhakaran MP, Jin G, et al. Polypyrrole-contained electrospun conductive nanofibrous membranes for cardiac tissue engineering. J Biomed Mater Res A 2011;99:376–385. DOI: 10.1002/jbm.a.33200
14. Wong JY, Langer R, Ingber DE. Electrically conducting polymers can noninvasively control the shape and growth of mammalian cells. Proc Natl Acad Sci U S A 1994;91:3201–3204.
15. Balint R, Cassidy NJ, Cartmell SH. Conductive polymers: Towards a smart biomaterial for tissue engineering. Acta Biomater 2014;10:2341–2353. DOI: 10.1016/j.actbio.2014.02.015
16. Ravichandran R, Sundarrajan S, Venugopal JR, et al. Applications of conducting polymers and their issues in biomedical engineering. J R Soc Interface 2010;7:S559–S579. DOI: 10.1098/rsif.2010.0120.focus
17. Bolto B, McNeill R, Weiss D. Electronic conduction in polymers. III. electronic properties of polypyrrole. Aust J Chem 1963;16:1090. DOI: 10.1071/CH9631090
18. Wise DL. Electrical and Optical Polymer Systems: Fundamentals, Methods, and Applications. Boca Raton, FL: CRC Press, 1998.
19. Liu X, Gilmore KJ, Moulton SE, et al. Electrical stimulation promotes nerve cell differentiation on polypyrrole/poly (2-methoxy-5 aniline sulfonic acid) composites. J Neural Eng 2009;6:065002. DOI: 10.1088/1741-2560/6/6/065002
20. Ghasemi-Mobarakeh L, Prabhakaran MP, Morshed M, et al. Application of conductive polymers, scaffolds and electrical stimulation for nerve tissue engineering. J Tissue Eng Regen Med 2011;5:e17–e35. DOI: 10.1002/term.383
21. Kaur G, Adhikari R, Cass P, et al. Electrically conductive polymers and composites for biomedical applications. RSC Adv 2015;5:37553–37567. DOI: 10.1039/C5RA01851J

22. Chiang CK, Fincher CR, Park YW, et al. Electrical conductivity in doped polyacetylene. Phys Rev Lett 1977;39: 1098–1101. DOI: 10.1103/PhysRevLett.39.1098
23. Wallace GG, Smyth M, Zhao H. Conducting electroactive polymer-based biosensors. TrAC Trends Anal Chem 1999; 18:245–251. DOI: 10.1016/S0165-9936(98)00113-7
24. Lee JW, Serna F, Nickels J, et al. Carboxylic acid-functionalized conductive polypyrrole as a bioactive platform for cell adhesion. Biomacromolecules 2006;7:1692–1695. DOI: 10.1021/bm060220q
25. Diaz AF, Kanazawa KK, Gardini GP. Electrochemical polymerization of pyrrole. J Chem Soc Chem Commun 1979;0:635. DOI: 10.1039/c39790000635
26. Tan Y, Ghandi K. Kinetics and mechanism of pyrrole chemical polymerization. Synth Met 2013;175:183–191. DOI: 10.1016/j.synthmet.2013.05.014
27. Guimard NK, Gomez N, Schmidt CE. Conducting polymers in biomedical engineering. Prog Polym Sci 2007;32: 876–921. DOI: 10.1016/j.progpolymsci.2007.05.012
28. Skotheim TA, Reynolds JR. Handbook of Conducting Polymers, 3e. Boca Raton, FL: CRC Press, 2007.
29. Sabouraud G, Sadki S, Brodie N, et al. The mechanisms of pyrrole electropolymerization. Chem Soc Rev 2000;29: 283–293. DOI: 10.1039/a807124a
30. Wang X, Gu X, Yuan C, et al. Evaluation of biocompatibility of polypyrrolein vitro andin vivo. J Biomed Mater Res 2004;68A:411–422. DOI: 10.1002/jbm.a.20065
31. Janmanee R, Chuekachang S, Sriwichai S, et al. Functional conducting polymers in the application of SPR biosensors. J Nanotechnol 2012;2012:1–7. DOI: 10.1155/2012/620309
32. Zhang Z, Rouabhia M, Wang Z, et al. Electrically conductive biodegradable polymer composite for nerve regeneration: Electricity-stimulated neurite outgrowth and axon regeneration. Artif Organs 2007;31:13–22. DOI: 10.1111/j.1525-1594.2007.00335.x
33. Kang TS, Lee SW, Joo J, et al. Electrically conducting polypyrrole fibers spun by electrospinning. Synth Met 2005;153:61–64. DOI: 10.1016/j.synthmet.2005.07.135
34. Liu H, Wang R, Chu HK, et al. Design and characterization of a conductive nanostructured polypyrrole-polycaprolactone coated magnesium/PLGA composite for tissue engineering scaffolds. J Biomed Mater Res A 2015;2966–2973. DOI: 10.1002/jbm.a.35428
35. Wan Y, Yu A, Hua W, et al. Porous-conductive chitosan scaffolds for tissue engineering II. In vitro and in vivo degradation. J Mater Sci Mater Med 2005;6:1017–1028.
36. Croisier F, Jérôme C. Chitosan-based biomaterials for tissue engineering. Eur Polym J 2013;49:780–792. DOI: 10.1016/j.eurpolymj.2012.12.009
37. Cui Z, Ni NC, Wu J, et al. Polypyrrole-chitosan conductive biomaterial synchronizes cardiomyocyte contraction and improves myocardial electrical impulse propagation. Theranostics 2018;8:2752–2764. DOI: 10.7150/thno.22599
38. He S, Song H, Wu J, et al. Preservation of conductive propagation after surgical repair of cardiac defects with a bio-engineered conductive patch. J Heart Lung Transplant 2018;37:912–924. DOI: 10.1016/J.HEALUN.2017.12.011
39. Bu Y, Xu HX, Li X, et al. A conductive sodium alginate and carboxymethyl chitosan hydrogel doped with polypyrrole for peripheral nerve regeneration. RSC Adv 2018;8: 10806–10817. DOI: 10.1039/c8ra01059e
40. Silva R, Singh R, Sarker B, et al. Soft-matrices based on silk fibroin and alginate for tissue engineering. Int J Biol Macromol 2016;93:1420–1431. DOI: 10.1016/j.ijbiomac.2016.04.045
41. Ouwerx C, Velings N, Mestdagh M, et al. Physicochemical properties and rheology of alginate gel beads formed with various divalent cations. Polym Gels Netw 1998;6:393–408. DOI: 10.1016/S0966-7822(98)00035-5
42. Venkatesan J, Bhatnagar I, Manivasagan P, et al. Alginate composites for bone tissue engineering: A review. Int J Biol Macromol 2015;72:269–281. DOI: 10.1016/j.ijbiomac.2014.07.008
43. Yang S, Jang L, Kim S, et al. Polypyrrole/alginate hybrid hydrogels: Electrically conductive and soft biomaterials for human mesenchymal stem cell culture and potential neural tissue engineering applications. Macromol Biosci 2016;16: 1653–1661. DOI: 10.1002/mabi.201600148
44. Sajesh KM, Jayakumar R, Nair SV, et al. Biocompatible conducting chitosan/polypyrrole-alginate composite scaffold for bone tissue engineering. Int J Biol Macromol 2013; 62:465–471. DOI: 10.1016/j.ijbiomac.2013.09.028
45. Green RA, Baek S, Poole-Warren LA, et al. Conducting polymer-hydrogels for medical electrode applications. Sci Technol Adv Mater 2010;11:014107. DOI: 10.1088/1468-6996/11/1/014107
46. Kundu B, Rajkhowa R, Kundu SC, et al. Silk fibroin biomaterials for tissue regenerations. Adv Drug Deliv Rev 2013;65:457–470. DOI: 10.1016/j.addr.2012.09.043
47. Murphy AR, Kaplan DL. Biomedical applications of chemically-modified silk fibroin. J Mater Chem 2009;19: 6443. DOI: 10.1039/b905802h
48. Rockwood DN, Preda RC, Yücel T, et al. Materials fabrication from Bombyx mori silk fibroin. Nat Protoc 2011;6: 1612–1631. DOI: 10.1038/nprot.2011.379.Materials
49. Hardy JG, Geissler SA, Aguilar D, et al. Instructive conductive 3D silk foam-based bone tissue scaffolds enable electrical stimulation of stem cells for enhanced osteogenic differentiation. Macromol Biosci 2015;15:1490–1496. DOI: 10.1002/mabi.201500171
50. Aznar-Cervantes S, Roca MI, Martinez JG, et al. Fabrication of conductive electrospun silk fibroin scaffolds by coating with polypyrrole for biomedical applications. Bioelectrochemistry 2012;85:36–43. DOI: 10.1016/j.bioelechem.2011.11.008
51. Romero IS, Schurr ML, Lally JV, et al. Enhancing the interface in silk–polypyrrole composites through chemical modification of silk fibroin. ACS Appl Mater Interfaces 2013;5:553–564. DOI: 10.1021/am301844c
52. Tsui JH, Ostrovsky-Snider NA, Yama DMP, et al. Conductive silk–polypyrrole composite scaffolds with bioinspired nanotopographic cues for cardiac tissue engineering. J Mater Chem B 2018;6:7185–7196. DOI: 10.1039/C8TB01116H
53. Murphy AR, John PS, Kaplan DL. Modification of silk fibroin using diazonium coupling chemistry and the effects on hMSC proliferation and differentiation. Biomaterials 2008;29:2829–2838. DOI: 10.1016/j.biomaterials.2008.03.039
54. Otero TF, Ariza MJ. Revisiting the electrochemical and polymeric behavior of a polypyrrole free-standing electrode in aqueous solution. J Phys Chem B 2003;107:13954–13961. DOI: 10.1021/jp0362842
55. Ren X, Pickup PG. Ion transport in polypyrrole and a polypyrrole/polyanion composite. J Phys Chem 1993;97: 5356–5362. DOI: 10.1021/j100122a029

56. Shang K, Rnjak-Kovacina J, Lin Y, et al. Accelerated in vitro degradation of optically clear low β-sheet silk films by enzyme-mediated pretreatment. Transl Vis Sci Technol 2013;2:2. DOI: 10.1167/tvst.2.3.2
57. Cao Y, Wang B. Biodegradation of silk biomaterials. Int J Mol Sci 2009;10:1514–1524. DOI: 10.3390/ijms10041514
58. Kim UJ, Park J, Joo KH, et al. Three-dimensional aqueous-derived biomaterial scaffolds from silk fibroin. Biomaterials 2005;26:2775–2785. DOI: 10.1016/j.biomaterials.2004.07.044
59. Yang J, Choe G, Yang S, et al. Polypyrrole-incorporated conductive hyaluronic acid hydrogels. Biomater Res 2016;20:31. DOI: 10.1186/s40824-016-0078-y
60. Wu T, Cui C, Huang Y, et al. Coadministration of an adhesive conductive hydrogel patch and an injectable hydrogel to treat myocardial infarction. ACS Appl Mater Interfaces 2020;12:2039–2048. DOI: 10.1021/acsami.9b17907.
61. Bueno VB, Takahashi SH, Catalani LH, et al. Biocompatible xanthan/polypyrrole scaffolds for tissue engineering. Mater Sci Eng C Mater Biol Appl 2015;52:121–128. DOI: 10.1016/j.msec.2015.03.023.
62. Yow S, Lim TH, Yim EKF, et al. A 3D electroactive polypyrrole-collagen fibrous scaffold for tissue engineering. Polymers (Basel) 2011;3:527–544. DOI: 10.3390/polym3010527
63. Wu C, Liu A, Chen S, et al. Cell-laden electroconductive hydrogel simulating nerve matrix to deliver electrical cues and promote neurogenesis. ACS Appl Mater Interfaces 2019;11:22152–22163. DOI: 10.1021/acsami.9b05520.
64. Hardy JG, Villancio-Wolter MK, Sukhavasi RC, et al. Electrical stimulation of human mesenchymal stem cells on conductive nanofibers enhances their differentiation toward osteogenic outcomes. Macromol Rapid Commun 2015;36:1884–1890. DOI: 10.1002/marc.201500233
65. Shafei S, Foroughi J, Stevens L. Electroactive nanostructured scaffold produced by controlled deposition of PPy on electrospun PCL. Res Chem Intermed 2017;43:1235–1251. DOI: 10.1007/s11164-016-2695-4
66. Vijayavenkataraman S, Kannan S, Cao T, et al. 3D-Printed PCL/PPy conductive scaffolds as three-dimensional porous nerve guide conduits (NGCs) for peripheral nerve injury repair. Front Bioeng Biotechnol 2019;7:266. DOI: 10.3389/fbioe.2019.00266
67. Gelmi A, Cieslar-Pobuda A, deMuinck E, et al. Direct Mechanical stimulation of stem cells: A beating electromechanically active scaffold for cardiac tissue engineering. Adv Healthc Mater 2016;5:1471–1480. DOI: 10.1002/adhm.201600307
68. Lee JY, Bashur CA, Goldstein AS, et al. Polypyrrole-coated electrospun PLGA nanofibers for neural tissue applications. Biomaterials 2009;30:4325–4335. DOI: 10.1016/j.biomaterials.2009.04.042
69. Zanjanizadeh N, Shahbazi M, Shatalin YV, et al. Conductive vancomycin-loaded mesoporous silica polypyrrole-based scaffolds for bone regeneration. Int J Pharm 2018;536:241–250. DOI: 10.1016/j.ijpharm.2017.11.065
70. Weng B, Liu X, Shepherd R, et al. Inkjet printed polypyrrole/collagen scaffold: A combination of spatial control and electrical stimulation of PC12 cells. Synth Met 2012;162:1375–1380. DOI: 10.1016/j.synthmet.2012.05.022
71. Adams A, VanDusen K, Kostrominova T, et al. Scaffold-less tissue-engineered nerve conduit promotes peripheral nerve regeneration and functional recovery after tibial nerve injury in rats. Neural Regen Res 2017;12:1529. DOI: 10.4103/1673-5374.215265
72. Ross CL, Zhou Y, McCall CE, et al. The use of pulsed electromagnetic field to modulate inflammation and improve tissue regeneration: A review. Bioelectricity 2019;1:247–259. DOI: 10.1089/bioe.2019.0026.
73. Levin M. Molecular bioelectricity: How endogenous voltage potentials control cell behavior and instruct pattern regulation in vivo. Mol Biol Cell 2014;25:3835–3850. DOI: 10.1091/mbc.E13-12-0708.
74. Pall ML. Electromagnetic fields act via activation of voltage-gated calcium channels to produce beneficial or adverse effects. J Cell Mol Med 2013;17:958–965. DOI: 10.1111/jcmm.12088.
75. Sundelacruz S, Moody AT, Levin M, et al. Membrane potential depolarization alters calcium flux and phosphate signaling during osteogenic differentiation of human mesenchymal stem cells. Bioelectricity 2019;1:56–66. DOI: 10.1089/bioe.2018.0005.
76. Cunha C, Panseri S, Antonini S. Emerging nanotechnology approaches in tissue engineering for peripheral nerve regeneration. Nanomed Nanotechnol Biol Med 2011;7:50–59. DOI: 10.1016/J.NANO.2010.07.004
77. Schmidt CE, Shastri VR, Vacanti JP, et al. Stimulation of neurite outgrowth using an electrically conducting polymer. Proc Natl Acad Sci U S A 1997;94:8948–8953.
78. Patel M, Min JH, Hong M-H, et al. Culture of neural stem cells on the conductive and microgrooved polymeric scaffolds fabricated via electrospun fiber-template lithography (EFTL). Biomed Mater 2020. [Epub ahead of print]; DOI: 10.1088/1748-605X/ab763b
79. Raynald R, Shu B, Liu XB, et al. Polypyrrole/polylactic acid nanofibrous scaffold cotransplanted with bone marrow stromal cells promotes the functional recovery of spinal cord injury in rats. CNS Neurosci Ther 2019;25:951–964. DOI: 10.1111/cns.13135.
80. Shu B, Sun X, Liu R, et al. Restoring electrical connection using a conductive biomaterial provides a new therapeutic strategy for rats with spinal cord injury. Neurosci Lett 2019;692:33–40. DOI: 10.1016/j.neulet.2018.10.031.
81. Bose S, Roy M, Bandyopadhyay A. Recent advances in bone tissue engineering scaffolds. Trends Biotechnol 2012;30:546–554. DOI: 10.1016/J.TIBTECH.2012.07.005
82. Khorshidi S, Karkhaneh A. Hydrogel/fiber conductive scaffold for bone tissue engineering. J Biomed Mater Res A 2018;106:718–724. DOI: 10.1002/jbm.a.36282
83. Leppik L, Zhihua H, Mobini S, et al. Combining electrical stimulation and tissue engineering to treat large bone defects in a rat model. Sci Rep 2018;8:6307. DOI: 10.1038/s41598-018-24892-0
84. Nicoll SB. Materials for bone graft substitutes and osseous tissue regeneration. In: Burdick JA, Mauck RL, eds. Biomaterials for Tissue Engineering Applications. Vienna: Springer, 2011: 343–362.
85. Pelto J, Björninen M, Pälli A, et al. Novel polypyrrole-coated polylactide scaffolds enhance adipose stem cell proliferation and early osteogenic differentiation. Tissue Eng Part A 2013;19:882–892. DOI: 10.1089/ten.tea.2012.0111
86. Ruvinov E, Sapir Y, Cohen S. Cardiac tissue engineering: Principles, materials, and applications. Synth Lect Tissue Eng 2012;4:1–200. Doi: 10.2200/S00437ED1V01Y201207TIS009

87. Chaudhuri R, Ramachandran M, Mohari LP, et al. Biomaterials and cells for cardiac tissue engineering: Current choices. Mater Sci Eng C 2017;79:950–957. DOI: 10.1016/j.msec.2017.05.121
88. Radisic M. Tissue engineering: Signals from within. Nat Mater 2016;15:596–597. DOI: 10.1038/nmat4648
89. Tarafder S, Bodhak S, Bandyopadhyay A, et al. Effect of electrical polarization and composition of biphasic calcium phosphates on early stage osteoblast interactions. J Biomed Mater Res B Appl Biomater 2011;97:306–314. DOI: 10.1002/jbm.b.31816.
90. van Vliet P, de Boer TP, van der Heyden MAG, et al. Hyperpolarization induces differentiation in human cardiomyocyte progenitor cells. Stem Cell Rev Rep 2010;6:178–185. DOI: 10.1007/s12015-010-9142-5.
91. Shevach M, Fleischer S, Shapira A, et al. Gold nanoparticle-decellularized matrix hybrids for cardiac tissue engineering. Nano Lett 2014;14:5792–5796. DOI: 10.1021/nl502673m
92. Kharaziha M, Shin SR, Nikkhah M, et al. Tough and flexible CNT-polymeric hybrid scaffolds for engineering cardiac constructs. Biomaterials 2014;35:7346–7354. DOI: 10.1016/j.biomaterials.2014.05.014
93. Vardharajula S, Ali SZ, Tiwari PM, et al. Functionalized carbon nanotubes: Biomedical applications. Int J Nanomedicine 2012;7:5361–5374. DOI: 10.2147/IJN.S35832
94. Song C, Zhang X, Wang L, et al. An injectable conductive three-dimensional elastic network by tangled surgical-suture spring for heart repair. ACS Nano 2019;13:14122–14137. DOI: 10.1021/acsnano.9b06761.
95. Zanjanizadeh EN, Ajdary R, Correia A, et al. Fabrication and characterization of drug-loaded conductive poly(glycerol sebacate)/nanoparticle-based composite patch for myocardial infarction applications. ACS Appl Mater Interfaces 2020;12:6899–6909. DOI: 10.1021/acsami.9b21066.

Address correspondence to:
James Cho-Hong Goh, PhD
Department of Biomedical Engineering
National University of Singapore
E3-05-18, 2 Engineering Drive 3
Singapore 117581
Singapore

E-mail: biegohj@nus.edu.sg